

Impact of hydrodynamic forces on a static vehicle at varying Froude numbers under partial submergence and subcritical flow conditions



Syed Muzzamil Hussain Shah, Zahiraniza Mustaffa*, Khamaruzaman Wan Yusof

Department of Civil and Environmental Engineering, Universiti Teknologi PETRONAS, 32610, Seri Iskandar, Perak, Malaysia

ARTICLE INFO

Article history:

Received 29 April 2019

Received in revised form

31 August 2019

Accepted 2 September 2019

Keywords:

Floodwaters

Hydrodynamic forces

Froude number

Static vehicle

Partial submergence

Subcritical flow

ABSTRACT

Roads are often the first assets affected by inundations which usually ends up as a serious hazard to the traffic. A vehicle, when submerged in floodwaters, is affected by several hydrodynamic forces, namely frictional, buoyancy, lift and drag forces. An understanding of the relevant forces involved is necessary to attempt to characterize the stability thresholds of vehicles in floodwaters. With that regards, a series of flume experiments were conducted on a static scaled model vehicle, Volkswagen Scirocco (1:24) which ensured the similarity laws. To assess the limiting thresholds that could lead to the stability failure modes, the vehicle was controlled to be partially submerged under the subcritical flow conditions. The vehicle was placed at the same domain with different orientations, namely 0°, 45°, 90°, 135°, 180°, 225°, 270°, 315° and 360° for each run to reduce inconsistencies in the test data. Based on the varying hydraulic variables assessed from the experimental runs, the hydrodynamic forces were theoretically estimated. Later, the relation between the hydrodynamic forces at varying Froude numbers was determined. From the study outcomes, an inverse relation of Froude number with respect to buoyancy force was noticed. On the other hand, an increment in the lift force slightly increased the Froude number. Similarly, a positive trend between the drag and frictional forces with respect to the Froude number was witnessed.

© 2019 The Authors. Published by IASE. This is an open access article under the CC BY-NC-ND license (<http://creativecommons.org/licenses/by-nc-nd/4.0/>).

1. Introduction

Flood related deaths are increasingly associated with people perishing in vehicles that become unstable while driving through floodwaters (Smith et al., 2019). Today, most of the major settlements of townships in many parts of the world are located along floodplains. With the continuing increase in urbanisation coupled with associated land development and encroachment activities, the natural form of the floodplains has significantly altered which often leads to the excessive flooding. Moreover, due to inadequate storm drainage system and the low-lying nature of these areas, the developed floodplains have been flooded frequently by many disastrous flooding events which have resulted in potential hazard risks to human life and

much damage has often occurred to the property and infrastructure (Teo et al., 2012a).

Floodwater is essentially a powerful component, strong enough to even move vehicles at the lowest hydraulic parameters (Martínez-Gomariz et al., 2018). A vehicle's stability would be compromised when the hydraulic variables exceed a certain limit, similar to the instability of pedestrians. However, in case of vehicles, characteristics like weight, aerodynamic shape, ground clearance and sealing capacity determines the level of stability in floodwaters (Shah et al., 2019). In the simplest terms, the damage and danger that floodwaters might cause to a vehicle could be related to the force of the flood flows as it travels down a floodplain. This force is generally described in terms of flow velocity and water depth ($v \times y$) (Smith, 2015).

To investigate the hydraulic variables, namely flow velocity (v) and water depth (y) that could lead to the stability failure of a static vehicle in floodwaters, laboratory physical experiments were conducted in the hydraulic flume located at University Technology PETRONAS (UTP), Malaysia. The vehicle was placed at the same domain with different orientations, namely 0°, 45°, 90°, 135°, 180°, 225°, 270°, 315° and 360° for each run to

* Corresponding Author.

Email Address: zahiraniza@utp.edu.my (Z. Mustaffa)

<https://doi.org/10.21833/ijaas.2019.11.006>

Corresponding author's ORCID profile:

<https://orcid.org/0000-0001-8002-8764>

2313-626X/© 2019 The Authors. Published by IASE.

This is an open access article under the CC BY-NC-ND license (<http://creativecommons.org/licenses/by-nc-nd/4.0/>)

reduce inconsistencies in the test data. The data points measured from the experimental investigation were then used to theoretically assess the hydrodynamic forces namely frictional, buoyancy, lift and drag forces. Later, the relation of these forces with respect to the Froude number has been conversed.

2. Background theory

Moving water, particularly floodwaters, create hydrodynamic forces. To assess the stability thresholds of vehicles in floodwaters, an understanding of the relevant forces, namely buoyancy, lift, drag and frictional forces is necessary to characterize the stability failure modes.

2.1. Buoyancy force (F_B)

Buoyancy force is an upward force exerted by a fluid that opposes the weight of the immersed object. In case of vehicles, when the buoyancy force exceeds vehicle weight, the vehicle starts to float and is carried away by the flow. This force can be expressed as:

$$F_B = \rho g V \quad (1)$$

where, ρ is the density of water, g is the acceleration due to gravity and V is the submerged volume of the vehicle (Shu et al., 2011).

2.2. Lift force (F_L)

The lift force is a component of a force which is flowing past the surface of a body and acts perpendicular to the incoming flow direction. It contrasts with the drag force, which is the component of the surface force parallel to the flow direction (Chien and Wan, 1999). The lift force can be expressed as:

$$F_L = \frac{1}{2} \rho C_L A_L v^2 \quad (2)$$

where, C_L is the lift coefficient, A_L is the acting area by the lift force which is given by $A_L = (l_c \times b_c)$ as shown in Fig. 1, where l_c and b_c are the length and width of the vehicle, respectively, and v is the flow velocity (Xia et al., 2011).

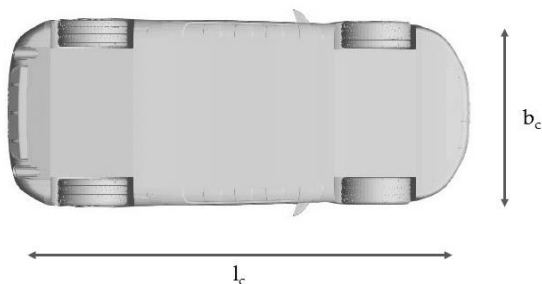


Fig. 1: Acting area by the lift force (A_L)

2.3. Drag force (F_D)

Drag force can be defined as resistance to moving through a fluid (Poirot, 2012). In fluid dynamics, drag acts opposite to the relative motion of any object moving with respect to a surrounding fluid. The drag force relies on the fluid density, drag coefficient, area of changing momentum and fluid velocity. It can be expressed as:

$$F_D = \frac{1}{2} \rho C_D A_D v^2 \quad (3)$$

where, C_D is the drag coefficient, A_D is the submerged area projected normal to the flow and v is the flow velocity (Teo et al., 2012b).

2.4. Frictional force (F_R)

Frictional force varies depending on the state of brakes being applied. However, once the vehicle is lifted off from the surface, the frictional force becomes zero. The general formula for the friction force can be expressed as:

$$F_R = \mu F_G \quad (4)$$

where, μ is the friction coefficient and F_G is the net weight of the vehicle (Teo et al., 2012b). The friction coefficient is simply a material property that relates to the two bodies involved and can be best estimated experimentally (Teo et al., 2012a).

3. Laboratory experimental setup

Laboratory physical experiments were conducted in the hydraulic flume of UTP. The flume is 10 m long, 0.45 m deep and 0.3 m wide, provided with a bed that can be adjusted to the desired slopes. Since the study was performed on a flat surface, the bed slope was kept at 0° . Today's vehicle on roads are different in design from the past, where new improvements in these vehicle design have taken into consideration. Therefore, in the current study a modern vehicle, Volkswagen Scirocco R with the geometric scale ratio of 1:24 was selected. The specifications of the prototype and model are shown in Fig. 2. Experiments were conducted to observe the limiting thresholds that would lead to the possibility of stability failure. With that regards, the discharge in the flume was adjusted gradually by means of valve, whereas the water depth was controlled through the vertical movement of wooden plank served as a sluice gate downstream of the flooded vehicle. As the flow approached the flooded vehicle, the velocity and water depth varied along the channel, therefore a certain section located at one vehicle length upstream of the flooded vehicle was assumed where the velocity and water depth were measured. This section was specified as representative of flow parameters acting on the vehicle (Xia et al., 2011). The model vehicle was placed at the same domain with different

orientations for each run to reduce inconsistencies in the test data. A point gauge attached to a roller (located at the top of the flume) was used to determine the water depths, whereas the approaching velocity was measured by using a portable velocity meter. A compact multi line laser

was also used to profoundly observe the instability of vehicle as it was uncertain to observe the vehicle movement in the water through naked eyes. Further, the instability points were visually recorded by means of a camcorder. The detailed schematic diagram of the experimental setup is shown in Fig. 3.

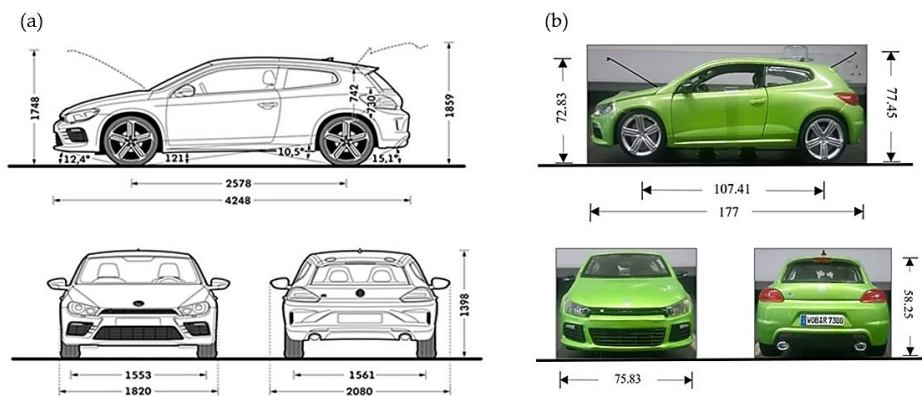


Fig. 2: Exterior dimensions (a) Prototype and (b) Model (1: 24)

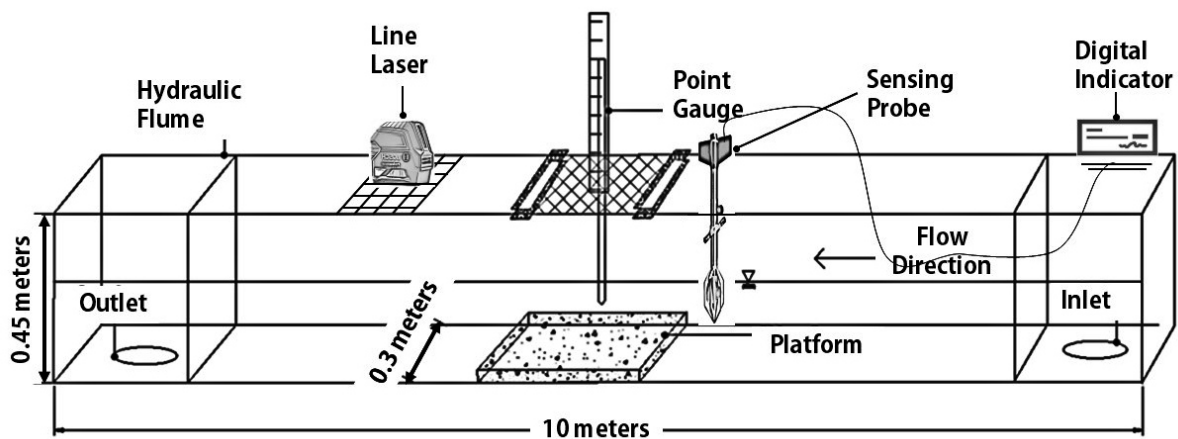


Fig. 3: Laboratory experimental setup

4. Theoretical assessment of hydrodynamic forces

Recall that for the estimation of buoyancy force (F_B), the submerged volume of the vehicle at different water depths (V), water density (ρ) and acceleration due to gravity (g) are required. Since ρ and g remains constant, therefore to estimate the buoyancy force, the submerged volume of the vehicle at different water depths was needed. Within that context, the chassis of the vehicle was precisely designed on scale (1:24) using AutoCAD. A two-dimensional design was initially prepared. The file was then saved as '*.dwg' format. It was then transferred to SolidWorks for further modification where the model was enhanced and extruded to prepare a complete three-dimensional chassis of the car. In contrast to the complex design of the chassis, the ring-shaped tire was simple to design as the diameter and width of the tire were known. Thus, the submerged volume of the tires at different water depths was separately determined. Herein the study was performed on a flat roadway condition under the subcritical flow conditions. Therefore, it was straight forward to estimate the submerged volume

of the car at the required water depths as it equally covered the vehicle chassis. Prior to crop the chassis at the desired depth, the ground clearance of the vehicle was also taken into consideration and it was ensured that the water depth was estimated exactly from the point where the tires were in contact to the ground. This file was then saved as '*.igs' format. Lastly, the saved file was then transferred to ANSYS (Static Structural) and the submerged volume of the vehicle at different water depths was obtained. Once the submerged volume of the chassis was known, it was then accumulated with the submerged volume of the tires for the estimation of buoyancy force.

The lift force (F_L) is a component of a vertical force which is flowing past the surface of a body that acts perpendicular to the direction of incoming flow. This contrasts with the drag force which is the component of the horizontal force that acts parallel to the direction of incoming flow. Recall that for the estimation of lift force, water density (ρ), lift coefficient (C_L), vertically projected area of the vehicle which is equivalent to the cross-sectional area of the car base (A_L) and the flow velocity are required. The lift coefficient can be determined if the distribution of the dynamic pressure and shear force

on the entire body are known. Pressure and shear forces are difficult to obtain along a surface for a non-geometry body either theoretically or experimentally and thus can only be obtained numerically (Salleh, 2009). Since ρ remains constant, therefore the value of C_L was obtained from the numerical simulations conducted on a similar car-type to observe the contribution of lift force to the incipient motion of a partly submerged flooded vehicle (Arrighi et al., 2015). In the current study, the proposed C_L value was considered as a reference value due to two main reasons: (i) both the studies were carried under partial submergence and (ii) the geometry of the city car considered for numerical simulations tallied well to the model vehicle tested in this study. Thus, the lift coefficient used to determine the lift force was selected as 0.45. Lastly, the plan area of the vehicle, A_L was considered when the water depth approaching the vehicle chassis exceeded the ground clearance. Once the water depth reached the bottom of the chassis, the vertically projected area of the vehicle remained constant and further increment in the water depth did not affect the cross-sectional area.

The drag force (F_D) on the vehicle is usually caused by the incoming flow which if exceeds the frictional force between the tires and the ground surface causes sliding instability failure. Unlike buoyancy force, which mainly relies on the submerged volume of the vehicle (V), the drag force depends on the submerged area projected normal to the flow (A_D), drag coefficient (C_D) and the approaching flow velocity (v). Therefore, the influence of drag force varies with vehicle position and the varying combination of hydraulic variables, i.e., (v - y) values. Herein ρ was taken as 1000 kg/m^3 , C_D was set to 1.1 or 1.15 depending on the depth of the floodwater level with respect to vehicle chassis (Xia et al., 2011) and v was experimentally determined at different water depths using the velocity meter. However, to estimate A_D , the

submerged volume of vehicle (V) was fractionated by the chassis width (b_c) at different water depths.

The friction force (F_R) concerns to the net weight of the vehicle (F_N) and the friction coefficient (μ). F_N is equivalent to vehicle weight in dry condition minus the vertical pushing force, namely buoyancy and lift forces, whereas μ depends on the tires condition and the roughness of the ground. For every increment in the water depth, the net weight of the vehicle was obtained once the buoyancy and lift forces were known. Moreover, for this study (static condition), the friction coefficient was assumed to be 0.3, which was confirmed almost adequate for the all the surface types as proposed by Bonham and Hattersley (1967).

5. Results and discussions

Flows in the flumes can be categorized as free surface flow which are generally driven both by gravity and inertia. Therefore, Froude number is the best correlation required to analyse the flow. On the other hand, Reynolds number deals with the relationship between frictional and inertial forces. For various reasons, the requirements posed by the Froude and Reynolds numbers cannot be satisfied simultaneously. It is then necessary to decide which the dominant forces are. Typically, free surface flows are governed by gravity forces, whereas Reynolds number effects (viscous drag) are most likely to become more significant at low Reynolds number (Mustaffa, 2004). However, under this section, an attempt has been made to study the relation of varying hydrodynamic forces with respect to the Froude number. At first, the relation of buoyancy force at varying Froude numbers has been discussed as shown in Fig. 4. The relationship of buoyancy force and Froude number is very straight forward. From the graph, it can be inferred that with the increasing Froude number, a decrease in the buoyancy force was noticed.

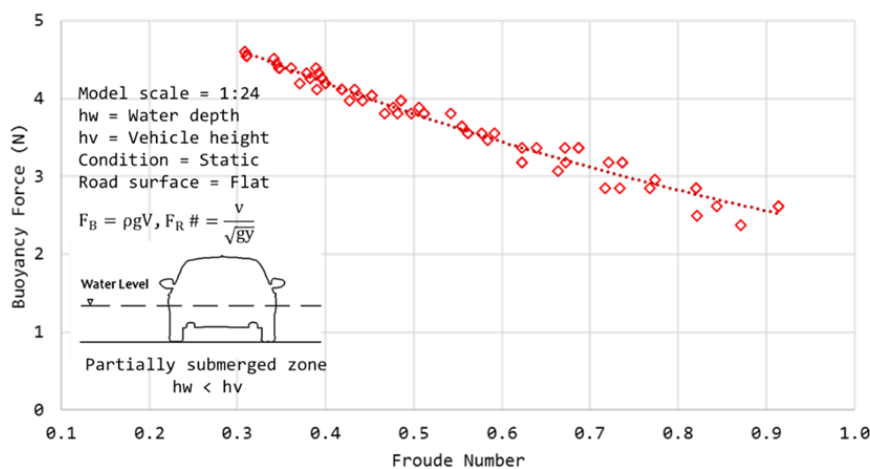


Fig. 4: Buoyancy force computed at varying Froude numbers

The buoyancy force solely relies on the submerged volume which varies with the water depth, whereas Froude number is inversely proportional to it. For instance, at the lowest Froude

number, the impact of buoyancy force was found maximum, whereas when the Froude number reached the maximum value, the buoyancy impact was found nominal. Based on these findings, it can be

concluded that Froude number is inversely proportional to the buoyancy force.

Likewise, the impact of buoyancy force, the impact of lift force relative to the Froude numbers has also been computed as shown in Fig. 5.

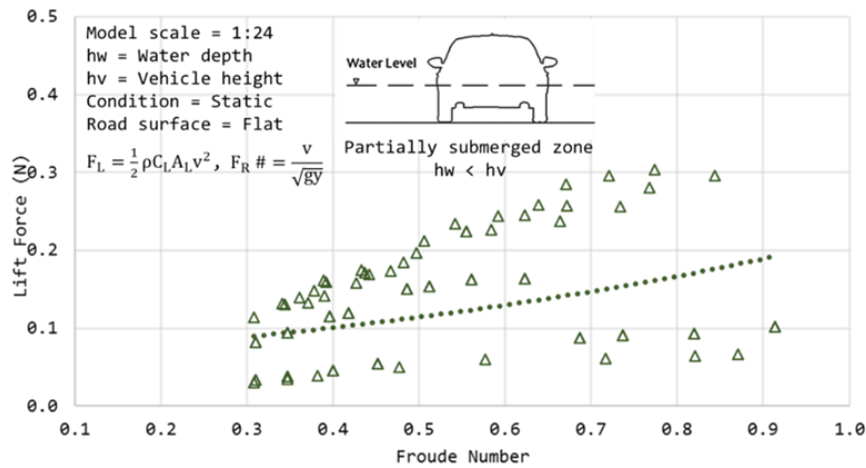


Fig. 5: Lift force computation at varying Froude numbers

The vertically projected area of the car, A_L remains constant as the floodwater depth reaches the vehicle chassis. Therefore, further increment in the water depth does not affect the plan area (A_L). On the other hand, the flow velocity is proportional to both lift force and the Froude number. Therefore, from the graph, it can be inferred that an increment in the lift force slightly increased the Froude number. Thus, a positive relation between the lift force and Froude number has been witnessed.

Drag force relies on the submerged area projected normal to the flow (A_D), which varies based on the level of submergence, position of vehicle towards the direction of incoming flow and the intensity of the flow at which it travels (v). A

pattern of gradual fluctuations in the drag force was noticed with an increase in the water depth. This highlights that drag force does not necessarily raise with the increasing water depth. However, referring to vehicle orientations, it can be seen that the influence of drag force was comparatively lower at the following orientations, namely 0° , 360° and 180° , as at these positions, the front and the rear ends of the vehicle were facing the incoming flow which provided smaller region to the drag force to take effect. However, the impact of drag force on the vehicle positioned at different angles, relative to Froude numbers has been further illustrated in Fig. 6.

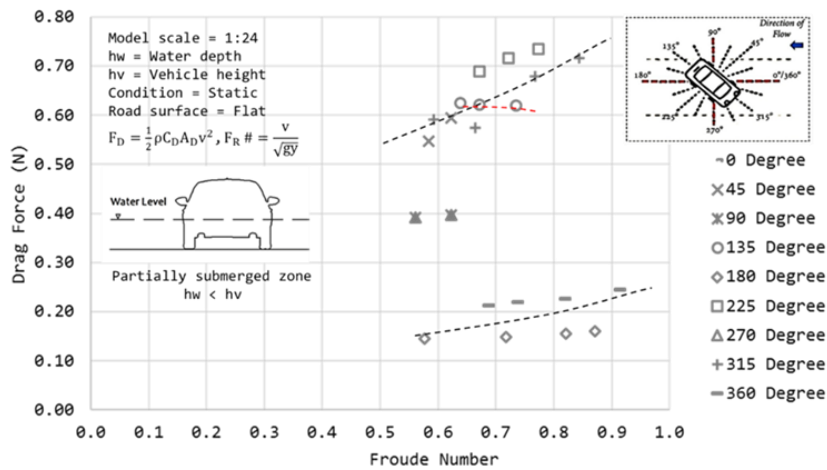


Fig. 6: Drag force computation at varying Froude numbers

From the above graph, it can be inferred that below the critical water depth, the influence of velocity was more dominant in contrast to shallow depths. For instance, at majority of the orientations, it was noticed that the increasing Froude number increased the impact of drag force on the vehicle. Though, it relies both on the varying combinations of

($v \cdot y$) values, but the graph concludes that at shallow depths, the flow velocity was more dominant to generate drag. Further, as highlighted earlier that drag varies with the vehicle orientation, thus, it can be seen that the influence of drag force differed nearly at the same Froude number for the vehicle at different orientations. For instance, at 0° , the impact

of drag force was noticed to be 0.23 N, when the value of Froude number reached 0.82. On the other hand, at 180°, the impact of drag force was noticed to be 0.15 N, for the same Froude number.

The buoyancy force takes effect immediately when a body is immersed in water and its impact becomes more intense as the water level goes up. This is suggested to be the major reason for the reduction in the frictional force under the given

circumstances. For instance, the maximum friction force between the vehicle tires and ground surface was found at the lowest water depth, i.e., 0.030 m, whereas at the maximum level (below critical water depth), i.e., 0.042 m, its influence was effectively reduced. Fig. 7 shows the relevance of friction force with respect to the Froude numbers so that the significance between the two can be studied.

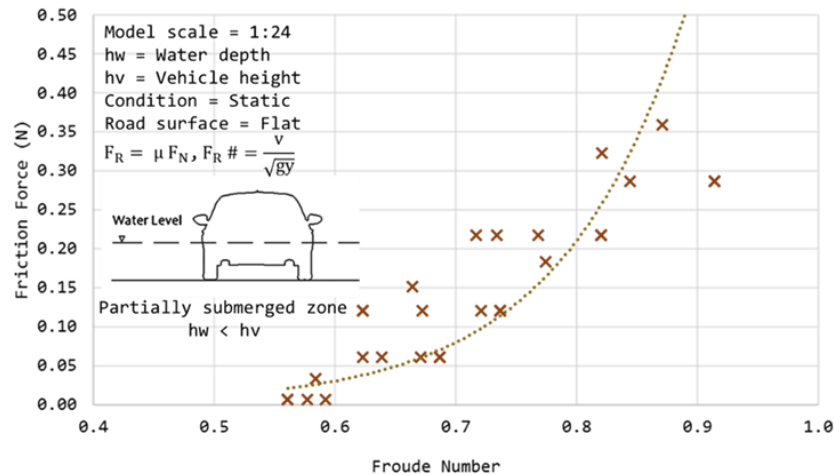


Fig. 7: Friction force computation at varying Froude numbers

The graph displays that the friction force is in proportion to the Froude number. It is straightforward because Froude number is inversely proportional to the water depth. So, for each increment in the water depth, the friction force is decreased and so does the Froude number. For instance, the impact of frictional force was found negligible at low Froude numbers, whereas it successively increased with the increasing Froude numbers.

6. Conclusion

The main findings of the study have highlighted that: (i) buoyancy force solely relies on the submerged volume which varies with the water depth, whereas the Froude number is inversely proportional to it. Thus, an inverse relation between the two was noticed, (ii) the lift force is concerned with the vehicle's vertical area of projection which is equivalent to the cross-sectional area of the car base (A_L) and the flow velocity (v). Notably, the affected area (A_L) does not vary once the water level reaches the chassis of the car. Thus, a positive relation between the lift force and Froude number has been witnessed, (iii) below the critical water depth, the influence of velocity was more dominant in contrast to shallow depths. For instance, at majority of the orientations, it was noticed that the increasing Froude number increased the impact of drag force on the vehicle. Though, it relies both on the varying combinations of ($v \cdot y$) values, but the outcomes conclude that at shallow depths, the flow velocity was more dominant to generate the drag. Thus, a positive trend between the two was noticed and (iv)

lastly, as the water depth goes up, the contact of the tires with the ground reduces. Since Froude number is inversely proportional to the water depth, therefore, a positive relation between the Froude number and friction force was noticed.

Acknowledgment

This research was supported by University Technology PETRONAS (UTP) Internal Grant (URIF 0153AAG24), the Prototype Fund Grant (Cost Centre: 015PBA-008) and the Technology Innovation Program (Grant No.: 10053121) funded by the Ministry of Trade, Industry and Energy (MI, Korea).

Compliance with ethical standards

Conflict of interest

The authors declare that they have no conflict of interest.

References

- Arrighi C, Alcèrrec-Huerta JC, Oumeraci H, and Castelli F (2015). Drag and lift contribution to the incipient motion of partly submerged flooded vehicles. *Journal of Fluids and Structures*, 57: 170-184. <https://doi.org/10.1016/j.jfluidstructs.2015.06.010>
- Bonham AJ and Hattersley RT (1967). Low level causeways. Technical Report No. 100, Water Research Laboratory, University of New South Wales, Kensington, Australia.
- Chien N and Wan Z (1999). *Mechanics of sediment transport*. American Society of Civil Engineers Press, Reston, USA. <https://doi.org/10.1061/9780784404003>

- Martínez-Gomariz E, Gómez M, Russo B, and Djordjević S (2018). Stability criteria for flooded vehicles: A state-of-the-art review. *Journal of Flood Risk Management*, 11(S2): S817-S826.
<https://doi.org/10.1111/jfr3.12262>
- Mustaffa Z (2004). An experimental investigation of the hydraulics of street inlets. M.Sc. Thesis, University of Alberta, Edmonton, Canada.
- Poirot S (2012). Handbook of fluid dynamics and fluid hydromonics: Fundamentals and applications. Auris Reference, London, UK.
- Salleh MKA (2009). Simulation and analysis drag and lift coefficient between sedan and hatchback car. Ph.D. Dissertation, Universiti Malaysia Pahang, Gambang, Malaysia.
- Shah SMH, Mustaffa Z, Martinez-Gomariz E, Kim DK, and Yusof KW (2019). Criterion of vehicle instability in floodwaters: Past, present and future. *International Journal of River Basin Management*: 1-41.
<https://doi.org/10.1080/15715124.2019.1566240>
- Shu C, Xia J, Falconer RA, and Lin B (2011). Incipient velocity for partially submerged vehicles in floodwaters. *Journal of Hydraulic Research*, 49(6): 709-717.
<https://doi.org/10.1080/00221686.2011.616318>
- Smith G (2015). Expert opinion: Stability of people, vehicles and buildings in flood water. Technical Report 2015/11, Water Research Laboratory, Allambie Heights, Australia.
- Smith GP, Modra BD, and Felder S (2019). Full-scale testing of stability curves for vehicles in flood waters. *Journal of Flood Risk Management*.
<https://doi.org/10.1111/jfr3.12527>
- Teo FY, Falconer RA, Lin B, and Xia J (2012a). Investigations of hazard risks relating to vehicles moving in flood. *The Journal of Water Resources Management*, 1(1): 52-66.
- Teo FY, Xia J, Falconer RA, and Lin B (2012b). Experimental studies on the interaction between vehicles and floodplain flows. *International Journal of River Basin Management*, 10(2): 149-160.
<https://doi.org/10.1080/15715124.2012.674040>
- Xia J, Teo FY, Lin B, and Falconer RA (2011). Formula of incipient velocity for flooded vehicles. *Natural Hazards*, 58(1): 1-14.
<https://doi.org/10.1007/s11069-010-9639-x>